Article

A neutralizing-protective supersite of human monoclonal antibodies for yellow fever virus
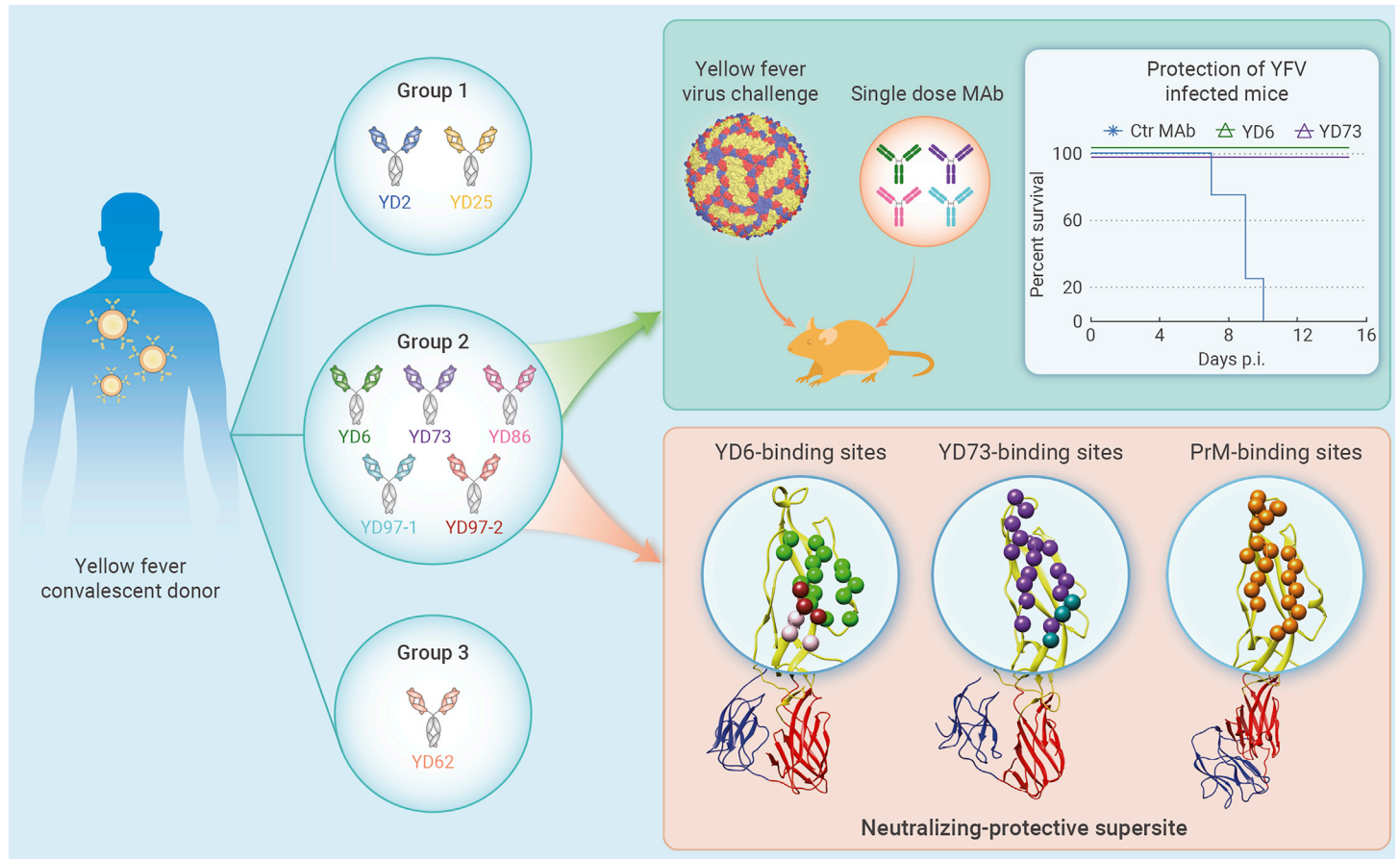
Yan Li,[1,8] Zhihai Chen,[2,8] Lili Wu,[1,8] Lianpan Dai,[1,3,4,8] Jianxun Qi,[1,3] Yan Chai,[1] Shihua Li,[1] Qihui Wang,[1] Zhou Tong,[1] Sufang Ma,[1] Xiaomin Duan,[1] Shuning Ren,[5] Rui Song,[2] Mifang Liang,[6] Wenjun Liu,[1] Jinghua Yan,[1,3,*] and George F. Gao[1,3,6,7,*]

*Correspondence: yanjh@im.ac.cn (J.Y.); gaof@im.ac.cn (G.F.G.)

GRAPHICAL ABSTRACT

PUBLIC SUMMARY

- Two monoclonal antibodies (mAbs, YD6 and YD73) have prophylaxis and therapy efficacy against the lethal challenge of YFV

- The crystal structures of mAbs bound to YFV envelope protein in pre-fusion and post-fusion conformations

- Two mAbs (YD6 and YD73) inhibit YFV infection at multiple steps

- The premembrane-binding region is a supersite recognized by YFV neutralizing mAbs

A neutralizing-protective supersite of human monoclonal antibodies for yellow fever virus

Yan Li,[1,8] Zhihai Chen,[2,8] Lili Wu,[1,8] Lianpan Dai,[1,3,4,8] Jianxun Qi,[1,3] Yan Chai,[1] Shihua Li,[1] Qihui Wang,[1] Zhou Tong,[1] Sufang Ma,[1] Xiaomin Duan,[1] Shuning Ren,[5] Rui Song,[2] Mifang Liang,[6] Wenjun Liu,[1] Jinghua Yan,[1,3,*] and George F. Gao[1,3,6,7,*]

[1]CAS Key Laboratory of Pathogen Microbiology and Immunology, Institute of Microbiology, Chinese Academy of Sciences, Beijing 100101, China
[2]Center of Infectious Disease, Beijing Ditan Hospital, Capital Medical University, Beijing 100015, China
[3]Savaid Medical School, University of Chinese Academy of Sciences, Beijing 101408, China
[4]Key Laboratory of Tropical Translational Medicine of Ministry of Education and School of Tropical Medicine and Laboratory Medicine, Hainan Medical University, Haikou, Hainan 571199, China
[5]College of Veterinary Medicine, China Agricultural University, Beijing 100193, China
[6]National Institute for Viral Disease Control and Prevention, Chinese Center for Disease Control and Prevention (China CDC), Beijing 102206, China
[7]Research Network of Immunity and Health, Beijing Institutes of Life Science, Chinese Academy of Sciences, Beijing 100101, China
[8]These authors contributed equally
*Correspondence: yanjh@im.ac.cn (J.Y.); gaof@im.ac.cn (G.F.G.)

The yellow fever virus (YFV) is a life-threatening human pathogen. Owing to the lack of available therapeutics, non-vaccinated individuals are at risk. Here, we isolated eight human monoclonal antibodies that neutralize YFV infection. Five recognized overlapping epitopes and exhibited potent neutralizing activity. Two (YD6 and YD73) were ultra-potent and conferred complete protection against the lethal challenge of YFV as both prophylactics and therapeutics in a mouse model. Crystal structures revealed that YD6 engaged the YFV envelope protein in both pre- and post-fusion states, suggesting viral inhibition by a "double-lock" mechanism. The recognition determinants for YD6 and YD73 are clustered at the premembrane (prM)-binding site. Notably, antibodies targeting this site were present in minute traces in YFV-infected individuals but contributed significantly to neutralization, suggesting a vulnerable supersite of YFV. We provide two promising candidates for immunotherapy against YFV, and the supersite represents an ideal target for epitope-based vaccine design.

INTRODUCTION

In recent years, there has been an unprecedented recurrence of flavivirus epidemics, including dengue fever, Zika disease, and yellow fever (YF).[1,2] The yellow fever virus (YFV) is the causative agent of YF and is a prototypical member of the *Flavivirus* genus of the *Flaviviridae* family. YFV infection can cause viral hemorrhagic disease with a case fatality rate of 15% to 50%.[3] Although the live-attenuated YFV vaccine has succeeded in preventing YF over the past decades,[4] non-vaccinated individuals are still at risk owing to incomplete vaccination coverage and contraindication for vaccine.[3,5] The recent years' outbreaks in Africa and South America led to hundreds of deaths, and also spilled over into China and the Netherlands (https://www.who.int/home/search?indexCatalogue=genericsearchindex1&searchQuery=yellow%20fever&wordsMode=AnyWord). The risk of YFV transmission is also increasing in the Asia-Pacific region, as the *Aedes aegypti* mosquitoes from these areas are vectors for YFV transmission and the exchanges between Africa and Asia are increasing.[6] To date, no effective therapeutics are available, highlighting the urgent need for the development of YFV therapeutics.

Protective monoclonal antibodies (mAbs) are a promising approach to prevent and treat viral infections, particularly for the coronavirus disease 2019 (COVID-19).[7-12] The flavivirus envelope (E) protein mediates viral entry into host cells and is the major target of protective antibodies.[13] E proteins bind to premembrane (prM) proteins as prM/E heterodimers on immature virions but form head-to-tail homodimers in the pre-fusion state on mature virions without pr peptides.[1] During viral infection, the E-dimer attaches to the cell membrane to initiate viral internalization into endosome. The conformation of E-dimer changes in the acidic endosome, exposing the hydrophobic fusion loop (FL) and E monomers rearranging in the plane of the viral membrane. The exposed FLs are then inserted into the endosomal membrane to promote trimer formation. Domain shifting and rotation trigger membrane fusion required for viral genome release.[14-16] To date, several mAbs have been reported to neutralize flavivirus infection at multiple stages of viral entry by inhibiting virus attachment and post-attachment steps.[12,17-19] Several mouse and human mAbs have been reported to neutralize YFV *in vitro*.[20,21] Only two neutralizing sites have been described: one in the FL for mAb 2A10G6 and the other, as we described previously, at the prM-binding site of DII for mAb 5A.[22] The mAb 5A functions as a "double lock" to neutralize YFV.[22] It binds to pre-fusion E-dimer to block virus attachment, entry, and E-dimer-to-trimer conformational changes. In addition, it binds to intermediate or post-fusion E-trimer to block virus-cell membrane fusion. However, the antigenic landscape for YFV neutralization remains to be elucidated.

In this study, we used soluble E protein (sE) as bait to isolate a panel of human mAbs from a YF convalescent. Eight mAbs neutralized YFV infection *in vitro*. Five exhibited potent activity (half maximal inhibitory concentration [IC_{50}] < 0.1 μg/mL) and were found to recognize overlapping epitopes, strongly suggesting a vulnerable site for neutralization. Among them, two antibodies, YD6 and YD73, displayed an ultra-potent neutralizing activity (IC_{50} < 0.01 μg/mL). Both YD6 and YD73 provided mice with pre- and post-exposure protection, even when administered as late as 4 days post infection (DPI). We further determined the crystal structures of YFV-sE in complex with YD6 and YD73, respectively. YD6 cross-linked E-dimers in a raft to lock them to the pre-fusion state. In addition, both YD6 and YD73 bound to E-trimer in its post-fusion state and sterically occluded FL insertion into the endosome membrane. Both YD6 and YD73 recognized epitopes clustered at the prM-binding site. Antibodies targeting this site were present in minute traces in the YFV-infected serum but contributed a substantial proportion of the neutralizing activity, suggesting an antigenic supersite as the "Achilles' heel" of YFV.

RESULTS

Isolation and characterization of human mAbs targeting YFV-E

Peripheral blood mononuclear cells (PBMCs) and serum samples were collected from four convalescents (designated C1–C4) with a YFV infection 6 months prior. The serum from C4 showed the highest neutralizing activity against YFV infection (Figures 1A and S1A); thus, we selected the PBMCs from C4 to screen for potent neutralizing antibodies. Using purified YFV-sE as bait, we isolated antigen-reactive single memory B cells from PBMCs using fluorescence-activated cell sorting (FACS) as described previously.[23,24] The variable gene regions of the antibodies (V_H and V_L) were amplified from the sorted single B cells and analyzed using the IMGT tool. Eight B cell receptors (BCRs) were paired from seven single cells, where two BCRs (YD97-1 and YD97-2) were sequenced from the same B cell with identical heavy chains as in YD73 but with distinct light chains (Table S1). The analysis of the germline gene usage of V_H suggested that these BCRs originated from six different B cell lineages, with the somatic hyper mutations ranging from 2 to 13 amino acid substitutions (Table S1).

The fragments of the variable region were then fused with the constant region of human immunoglobulin G1 (IgG1) to generate full-length mAbs for subsequent characterization. All eight mAbs bound to YFV-sE, and their binding affinities were further determined using real-time biophysical binding assays (BIAcore) (Figures 1D and S1B). Three mAbs, YD2, YD6, and YD73, exhibited strong binding
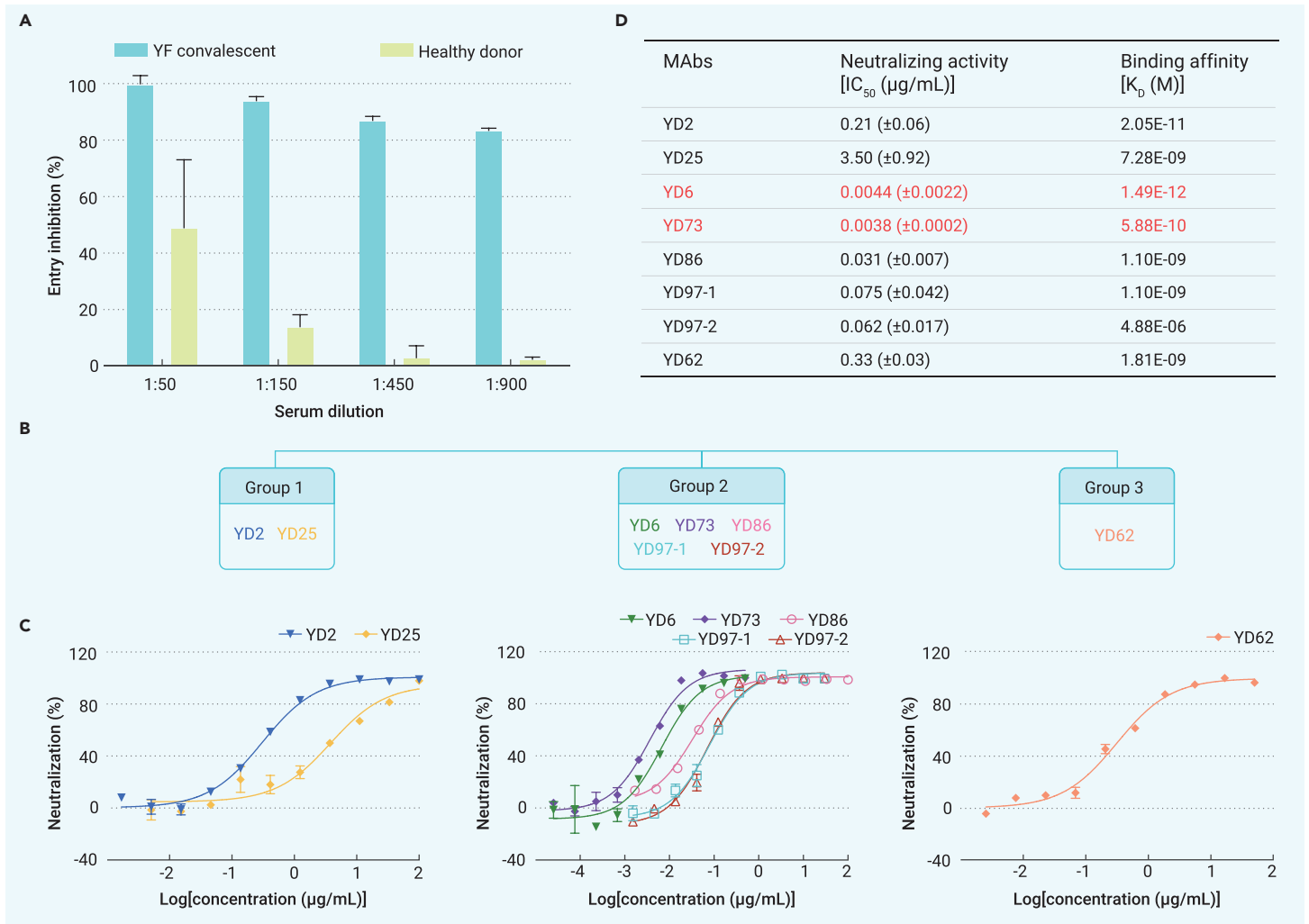
Figure 1. Neutralization activity, binding affinity, and mAb competition (A) The neutralization activity of serum against YFV CNYF01/2016 was evaluated with a flow cytometry-based neutralization assay. The serum was obtained from a YF convalescent infected with YFV 6 months ago; serum from a healthy donor was used as a control. Error bars indicate SD. (B) Graphics represent the binding competition among mAbs performed using an Octet RED96 biosensor (results are shown in Figures S2A and S2B). Isolated mAbs were classified into three groups according to their non-overlapping binding sites: group 1 (YD2 and YD25), group 2 (YD6, YD73, YD86, YD97-1, and YD97-2), and group 3 (YD62). (C) Neutralization activities of mAbs in the three groups against the YFV CNYF01/2016 strain were evaluated. Experiments were repeated three times. A single representative experiment is shown. Error bars indicate SD. (D) The average IC_{50} values with SD from three independent neutralization assays are listed in the middle line of the table. The two ultra-potent mAbs are highlighted. The interactions between sE and mAbs were monitored by surface plasmon resonance (SPR). The binding affinities (K_D) are listed in the right column of the table (graphics are shown in Figure S1).

affinities (K_D) to sE as 2.05×10^{-11} M, 1.49×10^{-12} M, and 5.88×10^{-10} M, respectively. In contrast, the other five mAbs displayed moderate or weak binding affinity, with K_D ranging from 4.88×10^{-6} to 1.10×10^{-9} M.

To further identify the recognition regions for these mAbs, binding competition assays were performed using Octet Red96. YD25 bound competitively with YD2 on sE, indicating that their epitopes shared an overlapping region, whereas the binding of the other six mAbs was not affected by YD2 (Figure S2A). The remaining six mAbs were further tested for binding competition with YD6. The binding of YD73 and YD86 to sE was obviously blocked by YD6, suggesting that these three mAbs recognized overlapping epitopes (Figure S2B). Owing to the low binding affinities of YD97-1 and YD97-2 to sE (Figures 1D and S1), we failed to determine the competition pattern for these two mAbs against YD6. Because of the same heavy chain usage for both YD97-1/-2 and YD73, we propose that they belong to the same competition group. YD62 did not compete with YD6 and was thus categorized into another group. As a result, these mAbs were classified into three major competition groups, designated as groups 1 to 3 (Figure 1B).

Neutralizing activities of the mAbs *in vitro*

To identify the neutralizing activity of the mAbs against YFV, we determined the IC_{50} values for each mAb using a modified FACS-based assay in Vero cells, as described previously.[24] All eight mAbs neutralized YFV (CNYF01/2016 strain) infection with distinctive potencies. MAbs in group 1 displayed weak or moderate

neutralizing activity, IC_{50} values of YD2 and YD25 were 0.21 μg/mL and 3.50 μg/mL, respectively (Figure 1C left panel and Figure 1D). Notably, all mAbs in group 2 exhibited potent neutralization ($IC_{50} < 0.1$ μg/mL), with IC_{50} values varying from 0.075 μg/mL to 0.0038 μg/mL. Importantly, YD6 and YD73 displayed neutralization in an ultra-potent range ($IC_{50} < 0.01$ μg/mL) with IC_{50} values of 0.0044 μg/mL and 0.0038 μg/mL, respectively (Figure 1C middle panel and Figure 1D). The only mAb in group 3, YD62, displayed moderate neutralizing activity (IC_{50} 0.33 μg/mL) (Figure 1C right panel and Figure 1D). Next, we assessed the cross-reactivity of two ultra-potent mAbs, YD6 and YD73, to other flaviviruses (dengue virus, West Nile virus, and Zika virus) using BIAcore assays. Clearly, both of them were YFV-specific (Figure S1B). As the most potent mAbs belonged to group 2, the antigenic site recognized by group 2 mAbs is likely a vulnerable site of YFV for antibody neutralization.

Prophylaxis and therapies of YD6 and YD73 against the lethal challenge of YFV *in vivo*

To evaluate the antiviral activity of YD6 and YD73 *in vivo*, we assessed the efficacy of these mAbs as pre- and post-exposure protection against YFV infection in a mouse model (Figures 2A–2D). The administration of 25 mg/kg of either YD6 or YD73 at 24 h after (Figures 2A and 2B) or 24 h before (Figures 2C and 2D) infection yielded 100% survival rates without signs of morbidity against the challenge with a lethal dose of YFV (CNYF01/2016). In contrast, mice without treatment or
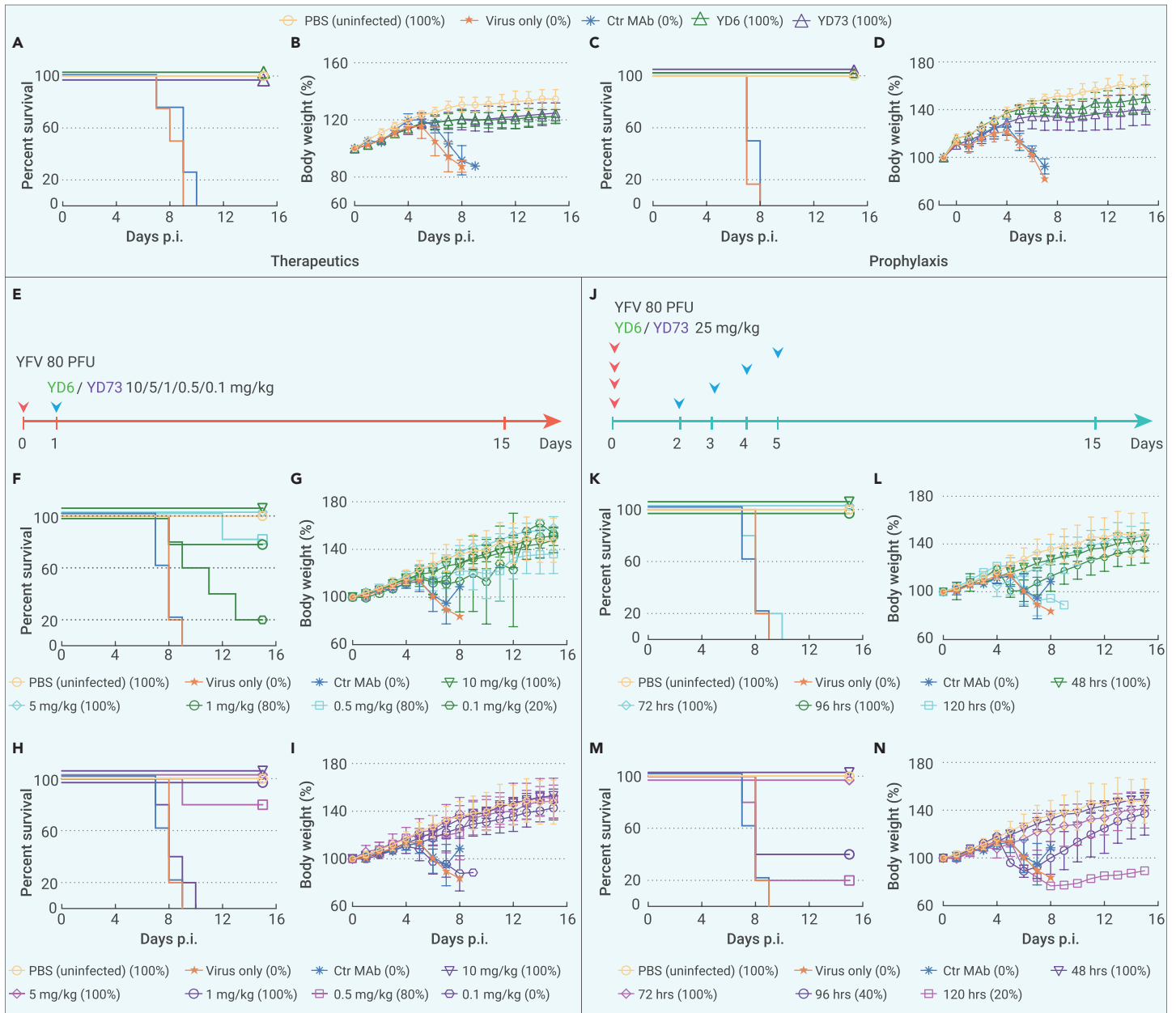
Figure 2. Therapeutic and prophylactic efficacies of YD6 and YD73 Three-week-old female mice were challenged with a lethal dose of YFV CNYF01/2016 strain. MAbs were subsequently administered pre- or post-challenge on the desired days and dosage as indicated. The Ebola-specific mAb 13C6 was used as a control (Ctr mAb). Mouse survival (A, C, F, H, K, and M) and body weight (B, D, G, I, L, and N) were monitored daily for 15 DPI. Error bars indicate SD. Survival rates as percentages are shown in parentheses, and the significance was analyzed using the log-rank test. (A and B) At 24 h post infection, 25 mg/kg of mAb was administered. Mouse survival (A) and body weight (B) were monitored. The significance of survival rates of both the YD6- and YD73-treated groups versus the Ctr-treated group was p = 0.0029 for both. (C and D) 25 mg/kg of mAb was administered 24 h in advance, the mice were infected, and survival (C) and body weight (D) were monitored. The significance of survival rates of the YD6- and YD73- treated groups versus the Ctr-treated group both was p = 0.0018 for both. (E) Scheme of the F−I experiment. Red arrow, challenge day; blue arrow, treatment day. (F−I) Mice were treated with YD6 (F and G) or YD73 (H and I) at 10, 5, 1, 0.5, and 0.1 mg/kg versus Ctr mAb at 25 mg/kg. The significances of the survival rates of the mAb-treated group versus the Ctr-treated group were calculated as follows: for YD6, 10, 5, and 0.5 mg/kg (p = 0.0019); 1 mg/kg (p = 0.011); 0.1 mg/kg (p = 0.023); for YD73, 10, 5, and 1 mg/kg (p = 0.0019); 0.5 mg/kg (p = 0.0048); and 0.1 mg/kg (p = 0.326). (J) Scheme of the K−N experiment. Red arrow, challenge day; blue arrow, treatment day. At 48, 72, 96, and 120 h post infection, 25 mg/kg YD6 (K, L) or YD73 (M, N) was administered. Mouse survival (K, M) and body weight (L, N) were monitored. The significances of the survival rates of the mAb-treated groups versus the Ctr-treated group were calculated as follows: for YD6, 48, 72, and 96 h (p = 0.0019); 120 h (p = 0.4419); for YD73, 48, and 72 h (p = 0.0019); 96 h (p = 0.0975); and 120 h (p = 0.4417).

receiving control mAb (13C6, an anti-Ebola virus mAb) succumbed to the YFV challenge between 7 and 10 DPI, with severe weight loss starting at 5 DPI (Figures 2A−2D).

To explore the minimal dosage required for efficient protection, mice were administered with 10, 5, 1, 0.5, or 0.1 mg/kg of YD6 or YD73 after the YFV challenge (Figures 2E−2I). Both YD6 (Figures 2F and 2G) and YD73 (Figures 2H and 2I) completely protected mice at minimum doses of 5 mg/kg and 1 mg/kg, respectively, and delayed morbidity and mortality even at the dose of 0.1 mg/kg (Figures 2F−2I).

In addition, we evaluated the therapeutic efficacy of these two mAbs at different time points after YFV exposure (Figure 2J). YD6 (Figures 2K and 2L) and YD73 (Figures 2M and 2N) were administered at 25 mg/kg as monotherapies to mice 48, 72, 96, and 120 h post-challenge with a lethal dose of YFV. Notably, YD6 treatment completely prevented mortality even when mAbs were administered at 96 h post-challenge, with body weights restored from 6 DPI (Figures 2K−2L). YD73 reduced mortality even when the mAb was administered at 120 h post-challenge (Figures 2M−2N). The high therapeutic activities of YD6 and YD73 *in vivo* suggest their potential for treating human YFV infections.

Article
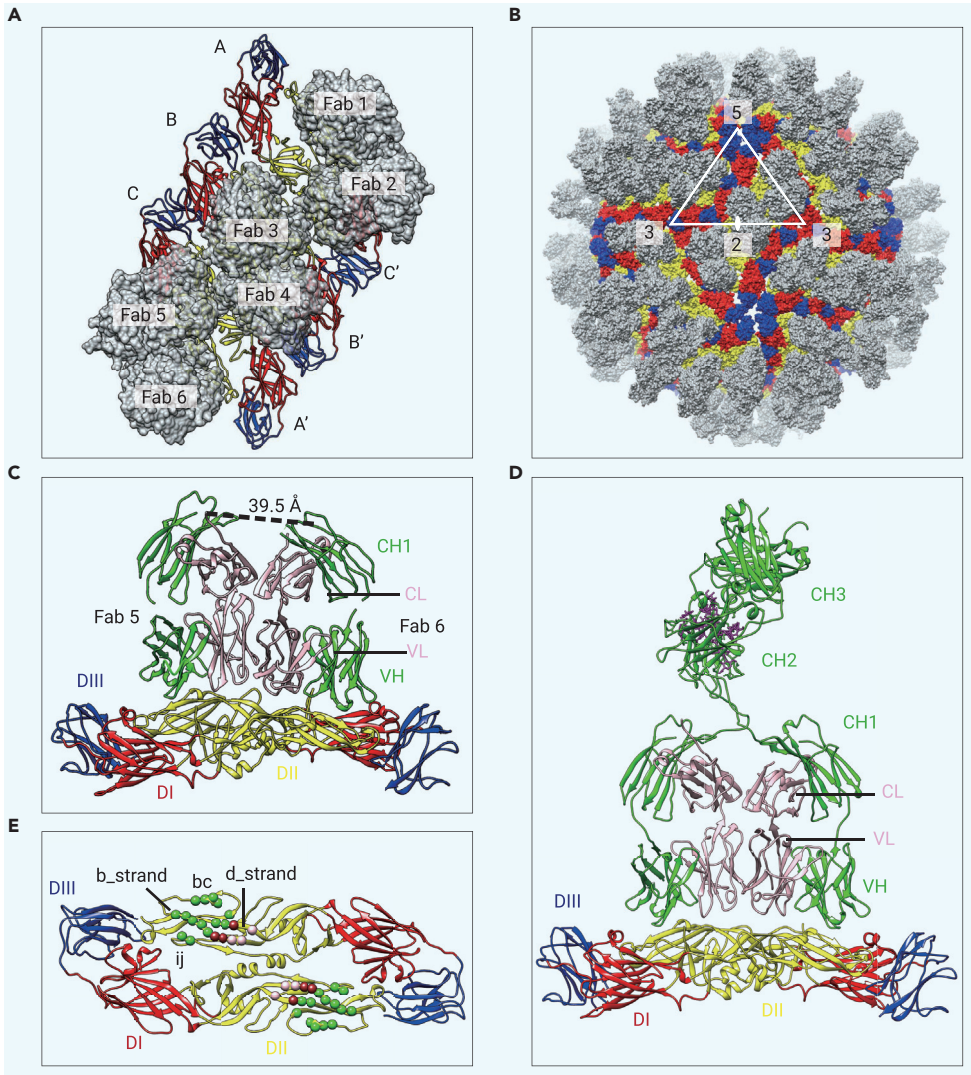
Figure 3. **The binding mode of YD6 to an E-dimer of YFV in the pre-fusion state** (A) The crystal structure of YD6 Fab in complex with YFV-sE. A "raft"-like structure of six E protomers bound to six YD6 Fabs in an asymmetric unit and are labeled as A, B, C, A′, B′, C′, and Fab1–6. E protomers are shown as ribbons. DI, DII, and DIII are colored in red, yellow, and blue, respectively. YD6 Fabs are colored in light gray and shown in surface representation. (B) Superimposing the complex of the YFV E-"raft" with the YD6 Fab onto the ZIKV particle model (PDB: 5IZ7). Proteins are shown as surface models with the domains and Fab colored as in (A). (C) The distances between adjacent Fabs (green and light pink ribbons for the heavy and light chains, respectively) in each E-dimer were measured. The close proximity between the CH1 domains of two Fabs (black line) indicates possible bivalent binding of IgG on the same virus particle. (D) Superimposition of a full IgG model on the complex structure of one E-dimer bound to two Fabs. (E) The residues of the YD6 epitope in the E-dimer are shown in spheres representation. The amino acids contacted by the heavy and light chains are colored in green and pink, respectively, with the overlapping residues in brown.

arrangement (Figure 3A). We superimposed the raft-like structure of YFV-E onto the Zika virus particle (PDB: 5IZ7) for comparison, and found that the raft-like structure from YFV-E/YD6 Fab structures was flatter than the raft in the Zika virus particle. When we superimposed the YD6 Fab in complex with the YFV E-dimer onto the Zika virus particle, 180 YD6 Fabs engaged 180 readily accessible epitopes on the exposed virion surface without sterically clashing or contact residues burying (Figure 3B).

The distances between two P213 Cα of Fab CH1 targeting an E-dimer are 39.5–46.0 Å, which are within a rational range of the hinge-bending motion of a full IgG. Concurrently, the distances between two Fab CH1 units in adjacent E-dimer are out of the range (Figures 3C and S4D).[7] Therefore, one YD6 may bridge an E-dimer on virus particles rather than two E proteins in neighboring E-dimers. We modeled YD6 as a full-length IgG in the Fab/sE complex structure, as previously described. The bivalent engagement of E protomers by the modeled IgG would lock the E-dimer in a pre-fusion state (Figure 3D).[7]

The epitope of YD6 is located on the fully exposed surface of DII in each E protomer (Figure 3E). The residues in the YD6 complementarity-determining regions of the heavy and light chains (HCDR and LCDR) have polar interactions with the residues in the a, b, d strands and *bc*, *ij* loops of DII in YFV-sE (Figure S4A and Table S3). In addition, the binding interface of YD6/sE displays clear shape and charge complementarity (Figure S5A). These data explain the high binding affinity of YD6 for sE.

Consistent with its infection-blocking activity at both pre- and post-attachment steps, the complete occupancy of the virion by YD6 would form an obstacle to virus attachment and hinder the conformational change of E proteins required for membrane fusion.

YD6 and YD73 inhibited viral infection at both pre- and post-attachment steps

Attachment of the virus to susceptible cells is the initial step in viral infection. To further characterize the mechanism of neutralization, we first examined whether YD6 and YD73 could block the cellular attachment of YFV using a method described previously.[23] The YFV mAb 5A, which has previously been demonstrated to block YFV attachment, was used as the positive control.[22] YFV was pre-incubated with Vero cells and then stained with the indicated mAbs. As expected, YD6, YD73, and 5A bound to YFV virions, exhibiting the fluorescence shifts (Figure S3A), whereas 13C6 did not bind to YFV virions. Thereafter, the virus particles were pre-incubated with the mAbs before incubation with Vero cells. Importantly, all of the mAbs reduced the fluorescence intensity to the baseline level, as displayed by cells without virus incubation, suggesting that both YD6 and YD73 inhibited virus attachment to the cells (Figure S3A).

We next explored whether YD6 and YD73 could neutralize the virus during the post-attachment step. YFV was incubated with dilutions of YD6 or YD73 before or after virus attachment to Vero cells. Viral infection was measured to evaluate neutralization activity.[7] We found that YD6 and YD73 effectively neutralized YFV infections at both pre- and post-attachment stages (Figure S3B). This tendency was similar to that previously reported for mAb 5A.[22]

Binding mode of YD6 to YFV E protein in the pre-fusion state

To dissect the molecular mechanism of neutralization, we crystallized the YD6 Fab in complex with YFV-sE. The crystal structure (Protein Data Bank [PDB]: 8GPU) was determined at 2.8 Å resolution (Table S2). An (sE/Fab) 6 complex is present in the asymmetric unit. Six Fabs bind to three E-dimers in a raft-like

Binding mode of YD6 and YD73 to E protein in the post-fusion state

Furthermore, protein complexes of YFV-sE bound to YD6 and YD73 were grown in acidic conditions, and the crystals were diffracted to a resolution of 3.1 Å and 3.8 Å, respectively (Table S2). In both structures(PDB: 8GPT, 8GPX), mAbs engage E-trimers in the post-fusion state (Figures 4A and 4B). The mAbs wrap the distal tip of the E-trimer and might cause a substantial steric hindrance for FL insertion into the target cell membrane resembling mAb 5A (Figures 4A–4C).[22] When the full IgG1(PDB:1HZH) molecules were superimposed onto the complex, they did not sterically clash with each other or with the E-trimer (Figure S5B).
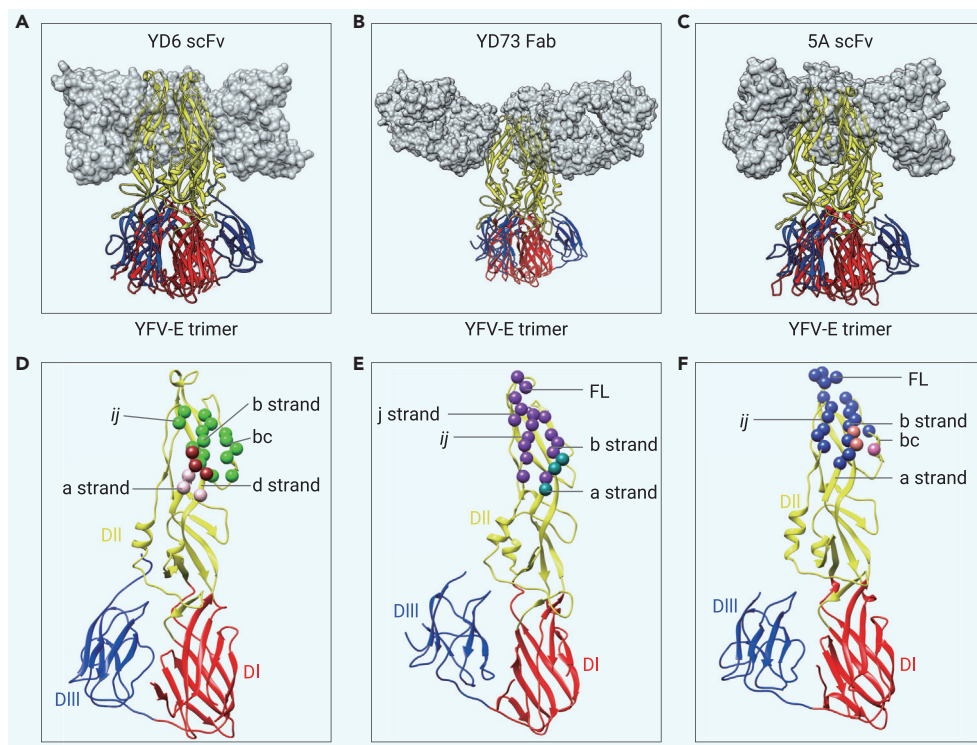
Figure 4. The binding modes of mAbs to an E-trimer of YFV in the post-fusion state (A–C) Side views of trimeric YD6scFv/sE (A), YD73 Fab/sE (B), and 5A scFv/sE (C). Three scFvs or Fabs bound to the post-fusional E-trimer, wrapping around the FLs. DI, DII, and DIII in the E-trimer are colored in red, yellow, and blue, respectively. scFvs or Fabs are colored in light gray and shown in surface representation. (D–F) The residues of the mAb epitope are labeled in spheres representation. (D) Residues interacting with the heavy and light chain of YD6 are colored in green and light pink, respectively. Those interacting with both the heavy and light chains are colored in brown. (E) Residues interacting with the YD73 heavy chain are colored in purple, and those interacted with both the heavy and light chains are colored in dark cyan. (F) Residues interacting with the heavy chain and light chain are colored in dark blue and hot pink, respectively, and those interacting with both the heavy and light chains are colored in salmon.

YD6 recognizes a completely exposed epitope in the post-fusion state (Figures 4A and 4D), similar to that in the pre-fusion state. Both the heavy and light chains of YD6 are involved in its interaction with DII of YFV-sE (Figure S4B). The interaction residues of YFV-sE in the a strand, b strand, *bc* loop, d strand, and *ij* loop at the post-fusion stage are consistent with those at the pre-fusion stage (Figure 4D and Table S4).
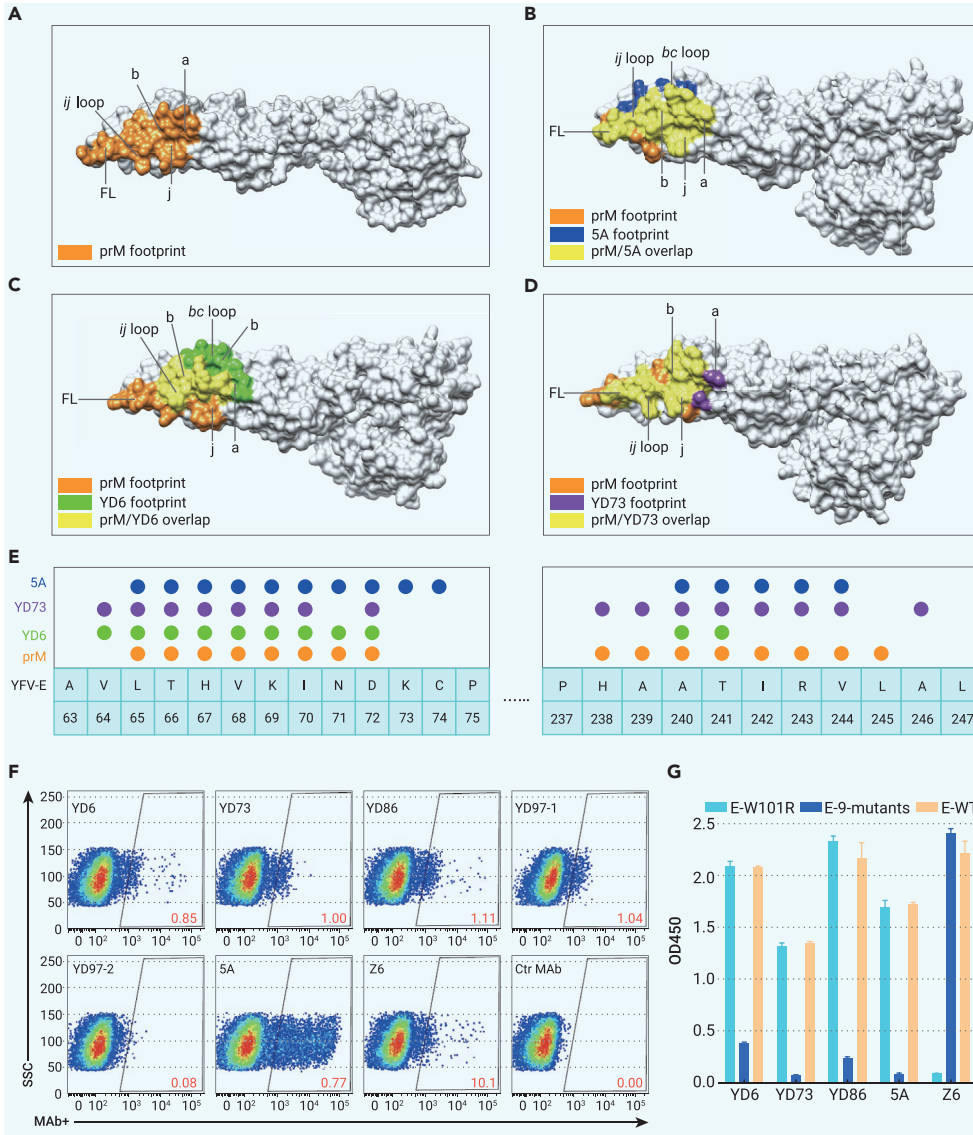
The epitope of YD73 mostly overlaps with that of YD6, including residues from the a and b strands, FL, and *ij* loop (Figures 4B, 4E, S4C, and S6, and Table S5). The surface electrostatic potential of the immunocomplex reveals the shape and charge complementarity at the binding interface (Figure S5A). When superimposed the structure of YD73/sE (post) onto YD6/sE (pre), we found that the epitope of YD73 was also fully exposed in the pre-fusion state of the E-dimer (Figure S5C), suggesting the attachment blockage by YD73. Given that YD6 and YD73 share highly overlapping epitopes with 5A (Figures 4D–4F), accordingly, they might neutralize YFV at multiple steps of virus entry via a "double-lock" mechanism.

MAbs in group 2 recognized the prM-binding site of YFV-E

The footprints of YD6, YD73, and 5A on the YFV-E are clustered at the end of the a strand, the entire b strand and part of the *ij* loop (Figures 4D–4F, S6, S7A, and S7B), representing a universal potent mAb recognition site. We analyzed the conservation of residues in contact with YD6, YD73, and 5A, respectively, and found that most residues were highly conserved among the 161 known YFV strains (Figure S7C), suggesting that YD6 and YD73, and 5A had broad neutralizing effects against YFV.

Further analysis shows that the footprints of YD6, YD73, and 5A are highly overlapped with that of prM on YFV 17D (Figures 5A–5D and S6) (YFV-prM/E PDB: 6EPK), including the b strand and *ij* loop. To confirm this finding, we stained the intracellular E protein in virus-infected cells with mAbs. The prM-binding sites should be occupied on the immature virus particle. Interestingly, we found YD6, YD73, 5A, and all other mAbs in group 2 stained poorly with intracellular E proteins (Figure 5F). In contrast, the FL-targeting mAb Z6[24] stained much higher populations of YFV-infected cells (Figure 5F).

We further substituted amino acids (64-VLTHVKIND-72) in the a and b strands shared in the epitopes of YD6, YD73, 5A, and prM-binding sites with those of ZIKV-E (64-SISDMASDS-72) (Figure 5E), designated as E-9-mutants. Neither group 2 mAbs nor 5A could bind to E-9-mutants but could bind to E-WT and E-W101R. In contrast, the mAb Z6 was able to engage

both E-9-mutants and E-WT but not E-W101R (Figure 5G). These findings supported that group 2 mAbs recognized the prM-binding site of YFV-E.

PrM-binding site was a supersite for YFV neutralization

To further characterize the antibodies targeting the prM-binding site in YFV-infected individuals, we first assessed their abundance in the serum samples. Sera from four convalescents with prior YFV infections were diluted and then incubated with the coated YFV E-W101R, E-9-mutants and E-WT, respectively. ELISAs were performed to measure the antigen-specific IgG levels. We found that antibodies binding to E-W101R were substantially decreased compared with E-WT; therefore, an estimated 40% to 60% of antibodies bound to YFV-E relied on W101 (Figure 6A) and likely targeted the FL, as previously reported.[27] In contrast, the amount of antibodies bound to E-9-mutants was almost equal to that bound to E-WT (Figure 6A), suggesting the minute traces of these antibodies in the sera.

Furthermore, the sera were adsorbed with E-W101R, E-9-mutants, E-WT, and control antigen (Ctr Ag), respectively (Figure S8), and antibodies bound to the corresponding antigens were depleted as previously described.[25] Thus, the antibodies left in the sera were those relying on W101 (mainly the FL epitope antibodies) for E-W101R adsorption,[12] or those relying on 64-VLTHVKIND-72 for E-9-mutant adsorption (Figure S8). After adsorption, the sera were tested for their binding properties to YFV E-WT by ELISA and for neutralizing activities against YFV infection.

Sera depleted by E-9-mutant beads showed almost equal levels of E-specific antibodies to those depleted by E-WT (Figure 6B), providing more evidence for the trace abundance of antibodies targeting 64-VLTHVKIND-72. In contrast, the amounts of the W101 antibodies were much higher, and the OD450 values of the E-W101R adsorbed group were 1.3- to 2.7-fold than those of the E-WT adsorbed group (Figure 6B). However, the neutralizing activities of the sera depleted by E-9-mutants were much higher (1.0- to 1.5-fold) than those depleted by E-W101R in C1, C3, and C4, and also higher (1.2- to 3.1-fold) than those depleted by E-WT in C1 to C4 (Figure 6C). These findings imply that, despite the trace amounts of the antibodies dependent on the prM-binding site in YFV-infected convalescents, they contributed a significant proportion of neutralization activity against YFV infection. Therefore, the prM-binding site is a vulnerable supersite of YFV.

DISCUSSION

To date, the antigenic landscapes for neutralizing antibodies have been examined in several flaviviruses, including Zika virus,[17] dengue virus,[19] and West Nile virus;[26] however, the antigenic epitopes of YFV remain elusive. We revealed a vulnerable supersite of YFV targeted by ultra-potent mAbs represented as group 2 antibodies and mAb 5A.[21,22] This site is localized at the prM-binding site on the E monomer with high conservation through YFV strains, implicating it as an ideal

Figure 5. Epitope comparison for YD6, YD73, 5A, and prM (A) Footprint of prM on YFV-sE. YFV-sE is shown as a surface model and colored in light gray, residues engaged by prM are colored in orange. (B–D) Footprints of 5A (B), YD6 (C), and YD73 (D) on YFV-sE at the post-fusion stage. The coloring corresponds to dark blue for 5A, green for YD6, purple for YD73, orange for prM, and yellow for overlap of prM with the indicated mAb. (E) Amino acids 63–75 and 237–247 of YFV-sE recognized by YD6, YD73, 5A, or prM are colored as indicated. E-9-mutants is the 64-VLTHVKIND-72 substituted by ZIKV-E 64-SISDMASDS-72. (F) Cells infected by YFV were permeated and stained with mAbs in group 2 (YD6, YD73, YD86, YD97-1, and YD97-2). 5A and Z6 were staining controls. Cells positive for mAb staining were detected by FACS. (G) ELISA detection for the binding of mAbs to coated YFV E-WT, E-W101R, and E-9-mutants. Error bars indicate SD.

with the viral membrane. The mAbs blocking FL insertion into the target membrane need further experiments for validation.

In this study, because soluble E was used as a bait, some antibodies recognizing quaternary epitopes, such as E-dimer epitope antibodies and "herringbone-specific" antibodies, may have been missed by this approach. In the future studies, screening approaches should be improved using mature virus particles for screening. In addition, mAbs with neutralizing potencies in the low ng/mL range have been identified for other flaviviruses to the site we described here and DIII in the E monomer,[28] E-dimer-specific epitopes,[8] and quaternary epitopes generated by the herringbone arrangement of E-dimers at the surface of flavivirus particles.[29] These studies suggested that this supersite is a continuum of antigenic sites that has the potential to induce highly potent antibodies. Finally, mAb YD2 has high affinity but poor neutralizing activity, because the neutralizing activity not only correlates with binding affinity but also with the recognizing epitope of E on the virion surface.

target for epitope-based vaccine design. Moreover, the antibodies targeting this site were present in trace amounts in the samples from the YFV-infected individuals, but contributed significantly to virus neutralization. Antibodies recognizing the prM-binding region have also been found in patients with dengue fever,[27] suggesting an attractive vaccine target against flavivirus infection. This finding opens a "door" for future research on flavivirus neutralization mechanism and immunodominance.

Flavivirus mAbs neutralize viral infections by several different mechanisms, including the aggregation of virus particles, destabilization of the virion structure, hindrance of virus attachment to host cells, and inhibition of membrane fusion.[7,19,22] A previous report demonstrated that the Zika virus mAb ZKA190 can bridge adjacent E proteins around the five- and three-fold axes.[7] Using the same modeling method, we found that two Fab arms of YD6 in a full IgG model could possibly lock an E-dimer, and 90 IgGs likely cross-linked 30 rafts in the prefusion state, YD6 and YD73 may hinder virus binding to cellular receptors. In addition, similar to the previously reported mAb 5A,[22] both YD6 and YD73 can engage YFV E proteins in the post-fusion states, thus might cause steric hindrance in the binding of FL to host cell membranes to inhibit virus entry via a "double-lock" mechanism. Therefore, our study delineates a new class of mAbs with a distinct neutralization mechanism for flavivirus.

There is a stem region peptide of E protein, anchored in the viral membrane, which passes very close to the epitope assigned in the post-fusion structure.[16] However, the truncated post-fusion trimers used in this study lack the region and do not represent the form that establishes the first interaction of the FL

The use of a clinically relevant challenge model is important for testing the therapeutics of mAbs. Because the mice neither lose weight nor die following YFV infection via the intraperitoneal route, we used intracranial infection instead to test the ability of antibodies to prevent mortality and proved the concept that the YD6 and YD73 could be potential therapeutic candidates. However, these data could not provide evidence of mAb treatment for viscerotropic disease caused by human YFV infection. In the future, the intervention of the mAbs after the onset of infection should be performed with more appropriate animals that exhibit viscerotropic disease, such as monkeys infected peripherally.

YFV remains a global threat to non-vaccinated individuals. In this study, both YD6 and YD73 were completely protective against YFV infection as post-exposure therapies, even administrated at 3 to 4 days post-challenge. Even at 5 DPI, YD73 reduced morbidity and mortality in mice. The onset of YF in humans occurs on day 3 to 6 after the virus infection. Therefore, these results suggest that both YD6 and YD73 might be an effective treatment in humans after the onset of YF, highlighting their feasibility in YFV immunotherapy; these findings need to be verified in clinical practice. In conclusion, we identified two mAb candidates with promising application in YF treatment and front-line defense for the susceptible populations.

MATERIALS AND METHODS

Materials and methods related to this work are available in the supplemental information.
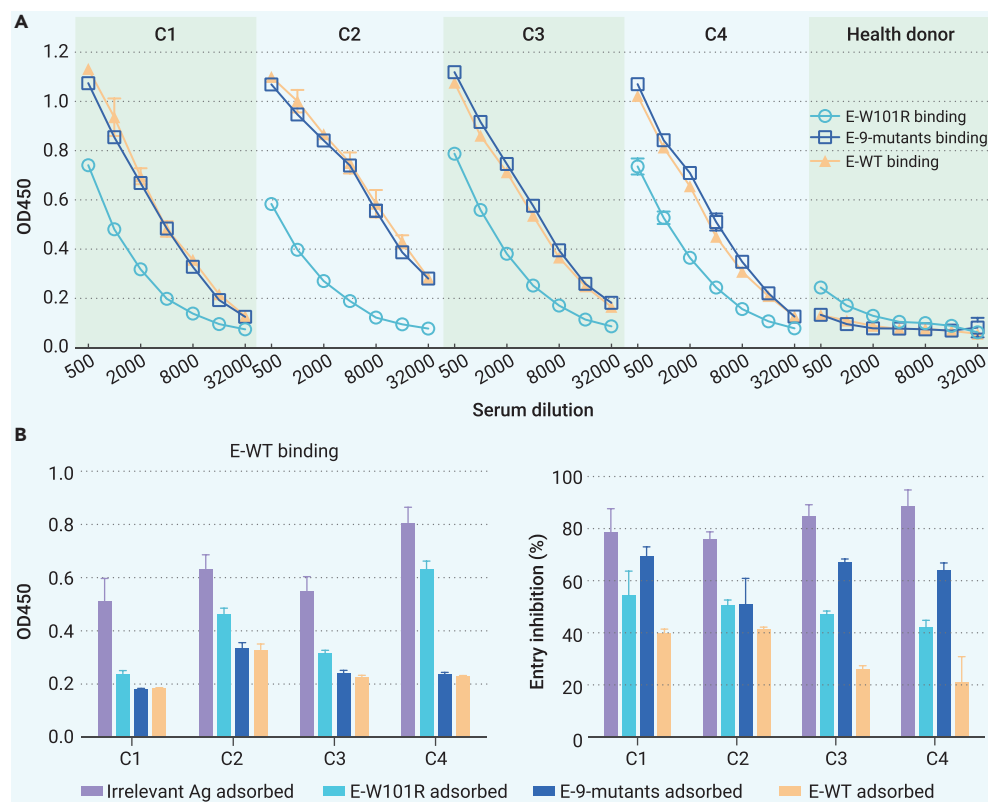
Figure 6. Antibodies targeting the prM-binding site play a key role in neutralization (A) Detection of the binding activity of the antibodies in sera to YFV E-WT, E-W101R, or E-9-mutants with ELISA. Sera were obtained from four YF convalescents (C1–C4) infected with YFV prior to 6 months; serum from a healthy donor was used as a control. Error bars indicate SD. (B) ELISA was performed to detect the binding of remaining antibodies in sera to YFV E-WT after E-WT, E-W101R, or E-9-mutants depletion. MERS-RBD was used as the negative control for the depletion assays (Ctr Ag). Error bars indicate SD. (C) Neutralization activities of sera after E-WT, E-W101R, or E-9-mutants depletion. Data are presented as the mean ± SD and are representative of three independent experiments. Error bars indicate SD.

DATA AVAILABILITY

The YFV-sE/YD6 Fab, YFV-sE/YD6 scFv, and YFV-sE/YD73 Fab structures in this study have been deposited in the PDB under accession numbers 8GPU, 8GPT, and 8GPX.

REFERENCES

1. Rey, F.A., Stiasny, K., Vaney, M.C., et al. (2018). The bright and the dark side of human antibody responses to flaviviruses: lessons for vaccine design. EMBO Rep. **19**, 206–224.
2. Gao, G.F. (2018). From "A"IV to "Z"IKV: attacks from emerging and re-emerging pathogens. Cell **172**, 1157–1159.
3. Elachola, H., Ditekemena, J., Zhuo, J., et al. (2016). Yellow fever outbreaks, vaccine shortages and the Hajj and Olympics: call for global vigilance. Lancet **388**, 1155.
4. Barrett, A.D.T. (2017). Yellow fever live attenuated vaccine: a very successful live attenuated vaccine but still we have problems controlling the disease. Vaccine **35**, 5951–5955.
5. Wilder-Smith, A. (2017). Yellow fever vaccination: estimating coverage. Lancet Infect. Dis. **17**, 1109–1111.
6. Lataillade, L.d.G.d., Vazeille, M., Obadia, T., et al. (2020). Risk of yellow fever virus transmission in the Asia-Pacific region. Nat. Commun. **11**, 5801.
7. Wang, J., Bardelli, M., Espinosa, D.A., et al. (2017). A human bi-specific antibody against Zika virus with high therapeutic potential. Cell **171**, 229–241.e15.
8. Barba-Spaeth, G., Dejnirattisai, W., Rouvinski, A., et al. (2016). Structural basis of potent Zika-dengue virus antibody cross-neutralization. Nature **536**, 48–53.
9. Wu, Y., Wang, F., Shen, C., et al. (2020). A noncompeting pair of human neutralizing antibodies block COVID-19 virus binding to its receptor ACE2. Science **368**, 1274–1278.
10. Shi, R., Shan, C., Duan, X., et al. (2020). A human neutralizing antibody targets the receptor binding site of SARS-CoV-2. Nature **584**, 120–124.
11. Baum, A., Fulton, B.O., Wloga, E., et al. (2020). Antibody cocktail to SARS-CoV-2 spike protein prevents rapid mutational escape seen with individual antibodies. Science **369**, 1014–1018.
12. Dejnirattisai, W., Wongwiwat, W., Supasa, S., et al. (2015). A new class of highly potent, broadly neutralizing antibodies isolated from viremic patients infected with dengue virus. Nat. Immunol. **16**, 170–177.
13. Dai, L., Song, J., Lu, X., et al. (2016). Structures of the Zika virus envelope protein and its complex with a flavivirus broadly protective antibody. Cell Host Microbe **19**, 696–704.
14. Mukhopadhyay, S., Kuhn, R.J., and Rossmann, M.G. (2005). A structural perspective of the flavivirus life cycle. Nat. Rev. Microbiol. **3**, 13–22.
15. Bressanelli, S., Stiasny, K., Allison, S.L., et al. (2004). Structure of a flavivirus envelope glycoprotein in its low-pH-induced membrane fusion conformation. EMBO J. **23**, 728–738.
16. Modis, Y., Ogata, S., Clements, D., and Harrison, S.C. (2004). Structure of the dengue virus envelope protein after membrane fusion. Nature **427**, 313–319.
17. Wang, Q., Yan, J., and Gao, G.F. (2017). Monoclonal antibodies against Zika virus: therapeutics and their implications for vaccine design. J. Virol. **91**, e01049-17–e01017.
18. Dai, L., Wang, Q., Qi, J., et al. (2016). Molecular basis of antibody-mediated neutralization and protection against flavivirus. IUBMB Life **68**, 783–791.
19. Fibriansah, G., and Lok, S.M. (2016). The development of therapeutic antibodies against dengue virus. Antivir. Res. **128**, 7–19.
20. Deng, Y.Q., Dai, J.X., Ji, G.H., et al. (2011). A broadly flavivirus cross-neutralizing monoclonal antibody that recognizes a novel epitope within the fusion loop of E protein. PLoS One **6**, e16059.
21. Daffis, S., Kontermann, R.E., Korimbocus, J., et al. (2005). Antibody responses against wild-type yellow fever virus and the 17D vaccine strain: characterization with human monoclonal antibody fragments and neutralization escape variants. Virology **337**, 262–272.
22. Lu, X., Xiao, H., Li, S., et al. (2019). Double lock of a human neutralizing and protective monoclonal antibody targeting the yellow fever virus envelope. Cell Rep. **26**, 438–446.e5.
23. Wang, Q., Ma, T., Wu, Y., et al. (2019). Neutralization mechanism of human monoclonal antibodies against Rift Valley fever virus. Nat. Microbiol. **4**, 1231–1241.
24. Wang, Q., Yang, H., Liu, X., et al. (2016). Molecular determinants of human neutralizing antibodies isolated from a patient infected with Zika virus. Sci. Transl. Med. **8**, 369ra179.
25. Ngwuta, J.O., Chen, M., Modjarrad, K., et al. (2015). Prefusion F-specific antibodies determine the magnitude of RSV neutralizing activity in human sera. Sci. Transl. Med. **7**, 309ra162.
26. Diamond, M.S., Pierson, T.C., and Fremont, D.H. (2008). The structural immunology of antibody protection against West Nile virus. Immunol. Rev. **225**, 212–225.
27. Rouvinski, A., Guardado-Calvo, P., Barba-Spaeth, G., et al. (2015). Recognition determinants of broadly neutralizing human antibodies against dengue viruses. Nature **520**, 109–113.
28. Robbiani, D.F., Bozzacco, L., Keeffe, J.R., et al. (2017). Recurrent potent human neutralizing antibodies to Zika virus in Brazil and Mexico. Cell **169**, 597–609.e11.
29. Zhang, S., Kostyuchenko, V.A., Ng, T.S., et al. (2016). Neutralization mechanism of a highly potent antibody against Zika virus. Nat. Commun. **7**, 13679.

DECLARATION OF INTERESTS

J.Y., G.F.G., Y.L., L.W., and S.M. are listed as the coinventors of the patents for the antibodies targeting envelope protein of yellow fever virus described in this study.

SUPPLEMENTAL INFORMATION

Supplemental information can be found online at https://doi.org/10.1016/j.xinn.2022.100323.

LEAD CONTACT WEBSITE

http://www.im.cas.cn/jgsz2018/yjtx/zgkxybywswymyxzdsys/202101/t20210120_5873142.html.